



# Robust Nonlinear Control of a Continuous Crystallizer

Timothy Chiu and Panagiotis D. Christofides

Department of Chemical Engineering, University of California, Los Angeles, CA 90095-1592, USA

**Abstract.** This paper proposes a nonlinear multivariable robust output feedback controller for a continuous crystallizer with fines trap which is modeled by a highly uncertain population balance model. Initially, the method of moments is applied to the population balance model to reduce it to a small set of differential equations, which is subsequently employed for controller synthesis by using a combination of geometric control methods with Lyapunov techniques. The performance and robustness of the proposed controller are successfully tested through simulations and are shown to be superior to the ones of a nonlinear controller which does not account for uncertainty.

**Key Words.** Population balance, Method of moments, Robust nonlinear control, Solution crystallization

## 1. Introduction

Crystallization is widely used in industry for the production of many high value products including fertilizers, proteins and pesticides and is characterized by highly nonlinear (owing to the Arrhenius dependence of nucleation laws on solute concentration) and oscillatory behavior (see the classic book (Randolph and Larson, 1988) for details and references). This suggests that crystallizers should operate under feedback control to ensure stable operation and attain a crystal size distribution with desired characteristics. This is very important because crystal size distribution influences significantly the necessary liquid-solid separation of the crystallizer effluent stream as well as the properties of the product and implies that crystallization requires a population balance in order to be accurately described, analyzed and controlled (Rawlings *et al.*, 1993).

Motivated by the importance and highly oscillatory nature of crystallization processes, there is a significant amount of literature on analysis and control of such processes. Specifically, significant previous efforts have focused on the understanding of fundamental control-theoretic properties (controllability and observability) of population balance models (e.g., (Semino and Ray, 1995a)) and the application of conventional (e.g. proportional-integral and proportional-integral-derivative control, self-tuning control) control schemes (see, for example, (Semino and Ray, 1995b; Rohani and Bourne, 1990) and the references therein). In (Eaton and Rawlings, 1990), an optimization-based control method was developed and successfully applied to a batch crystallization process. In a previous work (Chiu and Christofides, 1998), we developed a general method for the synthesis of nonlinear low-order output feedback controllers for particulate processes based on population balance models. These results on model-based control, coupled with recent developments in measurement technology which allow the ac-

curate and fast on-line measurement of key process variables including PSDs (see (Rawlings *et al.*, 1993) for an excellent review of the available measurement technology), are expected to significantly improve the operation of crystallization processes. Despite the recent progress on model-based control of crystallization processes, there are no available results on the synthesis of nonlinear controllers that explicitly account and compensate for the presence of uncertainty (e.g. unknown/partially known parameters and disturbances) in the process model.

This paper proposes a nonlinear multivariable robust output feedback controller for a continuous crystallizer with fines trap which is described by a highly uncertain population balance model. Initially, the method of moments is applied to the population balance model to reduce it to a small set of differential equations, which is subsequently used to synthesize the controller by using a combination of geometric control methods with Lyapunov techniques. The performance and robustness of the proposed controller are successfully tested through simulations and are shown to be superior to the ones of a nonlinear controller which does not account for uncertainty.

## 2. Crystallizer Description and Modeling

We consider a continuous crystallizer with fines trap shown in Figure 1 for which the following assumptions hold: isothermal operation, constant volume, mixed suspension, mixed product removal and nucleation of crystals of infinitesimal size. Application of a population balance to the particle phase and a mass balance to the continuous phase result in the following dynamic model for the crystallizer (Lei *et al.*, 1971):

$$\begin{aligned} \frac{\partial n}{\partial \bar{t}} &= -\frac{\partial(R(\bar{t})n)}{\partial r} - \frac{n}{\tau} - \bar{h}(r)\frac{n}{\bar{t}} + \delta(r-0)Q(\bar{t}) \\ \frac{dc}{d\bar{t}} &= \frac{(c_0 - \rho)}{\bar{\epsilon}\tau} + \frac{(\rho - c)}{\tau} + \frac{(\rho - c)}{\bar{\epsilon}} \frac{d\bar{\epsilon}}{d\bar{t}} \end{aligned} \quad (1)$$

where  $n(r, \bar{t})$  is the number of crystals of radius  $r \in [0, \infty)$  at time  $\bar{t}$  per unit volume of suspension,  $\tau$  is

the residence time,  $c$  is the solute concentration in the crystallizer,  $c_0$  is the solute concentration in the feed,  $\bar{\epsilon} = 1 - \int_0^\infty n(r, \bar{t}) \frac{4}{3} \pi r^3 dr$  is the volume of liquid per unit volume of suspension,  $R(\bar{t})$  is the growth rate,  $\delta(r - 0)$  is the standard Dirac function and  $Q(\bar{t})$  is the nucleation rate.  $1/\bar{\tau} = F_0/V$  is the rate at which crystals are circulated through the fines trap ( $F_0$  is the fines recirculation rate and  $V$  is the active volume of the crystallizer) and  $\bar{h}(r)$  expresses the desired selection curve for fines destruction (classification function). We assume that it is desirable to remove with the fines trap crystals of size  $r_m$  and smaller, and thus  $\bar{h}(r)$  takes the form:

$$\bar{h}(r) = \begin{cases} 1, & \text{for } r \leq r_m \\ 0, & \text{for } r > r_m \end{cases} \quad (2)$$

In the population balance, the term  $\delta(r - 0)Q(\bar{t})$  accounts for the production of crystals of infinitesimal (zero) size via nucleation.  $R(\bar{t})$  and  $Q(\bar{t})$  are assumed to follow McCabe's law and Volmer's nucleation law, respectively:

$$R(\bar{t}) = k_1(c - c_s), \quad Q(\bar{t}) = \bar{\epsilon} k_2 e^{-\frac{k_3}{\left(\frac{c}{c_s} - 1\right)^2}} \quad (3)$$

where  $k_1, k_2, k_3$  are constants and  $c_s$  is the concentration of solute at saturation. Using the expressions for  $Q(\bar{t})$  and  $R(\bar{t})$ , the system of Eq.1 can be written as:

$$\frac{\partial n}{\partial \bar{t}} = -k_1(c - c_s) \frac{\partial n}{\partial r} - \frac{n}{\bar{\tau}} - \bar{h}(r) \frac{n}{\bar{\tau}} - \frac{k_3}{\left(\frac{c}{c_s} - 1\right)^2} + \delta(r - 0) \bar{\epsilon} k_2 e^{-\frac{k_3}{\left(\frac{c}{c_s} - 1\right)^2}} \quad (4)$$

$$\frac{dc}{d\bar{t}} = \frac{(c_0 - \rho)}{\bar{\epsilon} \tau} + \frac{(\rho - c)}{\tau} + \frac{(\rho - c)}{\bar{\epsilon}} \frac{d\bar{\epsilon}}{d\bar{t}}$$

Owing to its distributed parameter nature, Eq.4 cannot be directly used for the synthesis of model-based feedback controllers. A model reduction procedure, which is outlined in the following section, will be used to reduce the system of Eq.4 into a small set of ordinary differential equations; which will be then used for the synthesis of robust nonlinear controllers.

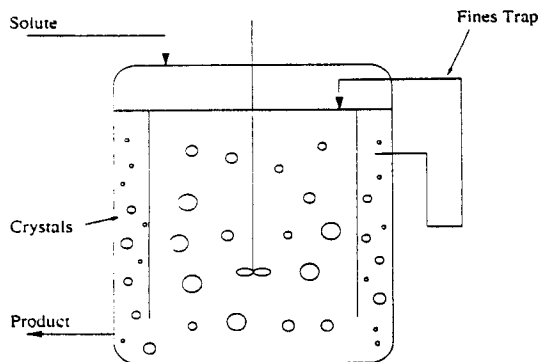


Fig. 1. A continuous crystallizer with fines trap.

### 3. Model Reduction

The model reduction procedure is based on a combination of the method of moments and the approximation of the particle size distribution with a Laguerre series expansion. This model reduction procedure is motivated from the fact that the dominant dynamics of the system of Eq.4 are characterized by a small number of degrees of freedom (Chiu and Christofides, 1998). Defining the  $\nu$ th moment of  $n(r, \bar{t})$  as:

$$\mu_\nu = \int_0^\infty r^\nu n(r, \bar{t}) dr, \quad \nu = 0, \dots, \quad (5)$$

multiplying the population balance in Eq.4 by  $r^\nu$  and integrating over all particle sizes, the following system of infinite ordinary differential equations, which describes the dynamics of the moments of the PSD and the solute concentration, is obtained:

$$\begin{aligned} \frac{d\mu_0}{d\bar{t}} &= -\frac{\mu_0}{\bar{\tau}} - \int_0^{r_m} \frac{n(r, \bar{t})}{\bar{\tau}} dr \\ &\quad + \left(1 - \frac{4}{3} \pi \mu_3\right) k_2 e^{-\frac{k_3}{\left(\frac{c}{c_s} - 1\right)^2}} \\ \frac{d\mu_\nu}{d\bar{t}} &= -\frac{\mu_\nu}{\bar{\tau}} + \nu k_1(c - c_s) \mu_{\nu-1} \\ &\quad - \int_0^{r_m} r^\nu \frac{n(r, \bar{t})}{\bar{\tau}} dr, \quad \nu = 1, 2, 3, \dots, \\ \frac{dc}{d\bar{t}} &= \frac{c_0 - c - 4\pi\tau(c - c_s)\mu_2(\rho - c)}{\tau \left(1 - \frac{4}{3} \pi \mu_3\right)} \end{aligned} \quad (6)$$

Referring to the above system, note that it constitutes an unclosed set of moment equations owing to the nature of the classification function of the fines destruction. An approximate analytical expression for  $n(r, \bar{t})$  in terms of the moments is needed in order to obtain a closed set of ordinary differential equations. Such an approximation using Laguerre polynomial expansion was suggested in (Hulburt and Katz, 1964) and takes the following form:

$$n(r, \bar{t}) = \frac{\lambda}{a} p^{(\lambda)} \left( \frac{\lambda r}{a} \right) \sum_{n=0}^{\infty} k_n L_n^{(\lambda)} \left( \frac{\lambda r}{a} \right) \quad (7)$$

where  $a$  and  $\lambda$  are functions of the moments of the particle size distribution which are explicit functions of time.  $L_n^{(\lambda)}$  are the  $n^{\text{th}}$  order Laguerre polynomials:

$$L_n^{(\lambda)}(z) = \sum_{j=0}^n (-1)^j \frac{n!(n + \lambda - 1)!}{j!(n - j)!(n + \lambda - 1 - j)!} z^{n-j} \quad (8)$$

$$n = 0, 1, 2, \dots$$

which are constructed by orthogonalizing the powers of  $z$  with respect to the  $\Gamma$ -distribution weighting function:

$$p^{(\lambda)}(z) = \frac{1}{(\lambda - 1)!} z^{\lambda-1} e^{-z} \quad (9)$$

and  $k_n$  takes the following form:

$$k_n = \sum_{j=0}^n (-1)^j \frac{(\lambda - 1)!}{j!(n + \lambda - 1 - j)!} \frac{(\lambda/a)^{n-j}}{(n - j)!} \mu_{n-j} \quad (10)$$

with the leading terms of  $k_n$  being:

$$\begin{aligned} k_0 &= \mu_0 \\ k_1 &= \frac{1}{a}\mu_1 - \mu_0 \\ k_2 &= \frac{1}{2a^2}\frac{\lambda}{\lambda+1}\mu_2 - \frac{1}{a}\mu_1 + \frac{1}{2}\mu_0 \end{aligned} \quad (11)$$

If we choose  $a$  and  $\lambda$  to be:

$$a = \frac{\mu_1}{\mu_0} \quad \lambda = \frac{a^2}{\mu_2/\mu_0 - a^2} \quad (12)$$

so as to force  $k_1$  and  $k_2$  to be 0, Eq.7 becomes:

$$n(r, \bar{t}) = \frac{\lambda}{a} p^{(\lambda)} \left( \frac{\lambda r}{a} \right) \left[ \mu_0 + \sum_{n=3}^{\infty} k_n L_n^{(\lambda)} \left( \frac{\lambda r}{a} \right) \right] \quad (13)$$

Neglecting the terms in Eq.13 with  $n = 3$  and higher results in the following approximation for the particle size distribution:

$$n(r, \bar{t}) = \frac{\lambda(\bar{t})}{a(\bar{t})} p^{(\lambda(\bar{t}))} \left( \frac{\lambda(\bar{t})r}{a(\bar{t})} \right) \mu_0 \quad (14)$$

Substituting Eq.14 into Eq.6 and introducing the following set of dimensionless variables and parameters:

$$\begin{aligned} t &= \frac{\bar{t}}{\tau}, \quad \bar{x}_0 = 8\pi\sigma^3\mu_0, \quad \bar{x}_1 = 8\pi\sigma^2\mu_1, \quad \bar{x}_2 = 4\pi\sigma\mu_2, \\ \bar{x}_3 &= \frac{4}{3}\pi\mu_3, \dots, \quad \sigma = k_1\tau(c_0 - c_s), \\ Da &= 8\pi\sigma^3k_2\tau, \quad F = \frac{k_3c_s^2}{(c_0 - c_s)^2}, \quad \alpha = \frac{(\rho - c_s)}{(c_0 - c_s)} \end{aligned} \quad (15)$$

$$\bar{y} = \frac{(c - c_s)}{(c_0 - c_s)}$$

the following system is obtained:

$$\begin{aligned} \frac{d\bar{x}_0}{dt} &= -\bar{x}_0 + (1 - \bar{x}_3)Da\epsilon \frac{-F}{\bar{y}^2} \\ &\quad - 8\pi\sigma^3\mu_0 \frac{\tau}{\bar{r}} \frac{1}{(\lambda - 1)!} \left( \frac{\lambda}{a} \right)^\lambda \int_0^{r_m} r^{\lambda-1} e^{-\frac{\lambda r}{a}} dr \\ \frac{d\bar{x}_1}{dt} &= -\bar{x}_1 + \bar{y}\bar{x}_0 \\ &\quad - 8\pi\sigma^2\mu_0 \frac{\tau}{\bar{r}} \frac{1}{(\lambda - 1)!} \left( \frac{\lambda}{a} \right)^\lambda \int_0^{r_m} r^{\lambda} e^{-\frac{\lambda r}{a}} dr \\ \frac{d\bar{x}_2}{dt} &= -\bar{x}_2 + \bar{y}\bar{x}_1 \\ &\quad - 4\pi\sigma\mu_0 \frac{\tau}{\bar{r}} \frac{1}{(\lambda - 1)!} \left( \frac{\lambda}{a} \right)^\lambda \int_0^{r_m} r^{\lambda+1} e^{-\frac{\lambda r}{a}} dr \\ \frac{d\bar{x}_3}{dt} &= -\bar{x}_3 + \bar{y}\bar{x}_2 \\ &\quad - \frac{4}{3}\pi\mu_0 \frac{\tau}{\bar{r}} \frac{1}{(\lambda - 1)!} \left( \frac{\lambda}{a} \right)^\lambda \int_0^{r_m} r^{\lambda+2} e^{-\frac{\lambda r}{a}} dr \\ &\vdots \\ \frac{d\bar{y}}{dt} &= \frac{1 - \bar{y} - (\alpha - \bar{y})\bar{y}\bar{x}_2}{1 - \bar{x}_3} \end{aligned} \quad (16)$$

On the basis of the system of Eq.16, it is clear that

the moments of order four and higher do not affect those of order three and lower, which means that the dominant dynamics of the system of Eq.6 can be adequately captured by the first four moment equations and the mass balance equation of Eq.16. This fifth-order ODE system will be used to synthesize a robust nonlinear feedback controller for the crystallizer in the next section.

#### 4. Controller synthesis

The multivariable control problem is formulated as the one of controlling the particle number concentration and the solute concentration, i.e.:

$$\begin{aligned} y_1(\bar{t}) &= 8\pi\sigma^3 \int_0^{\infty} n(r, \bar{t}) dr = \bar{x}_0, \\ y_2(\bar{t}) &= \frac{(c(\bar{t}) - c_s)}{(c_0 - c_s)} = \bar{y}(\bar{t}) \end{aligned} \quad (17)$$

by manipulating the flow rate of suspension through the fines trap and the inlet solute concentration, i.e.:

$$\bar{u}_1(\bar{t}) = \frac{1}{\bar{\tau}} - \frac{1}{\bar{\tau}_s}, \quad \bar{u}_2(\bar{t}) = \frac{c_0 - c_0_s}{c_0 - c_s} \quad (18)$$

where  $1/\tau_s$  and  $c_0_s$  denote the circulation rate of suspension in the fines trap and the inlet concentration at steady state, respectively. Uncertainties in the form of modeling errors in the pre-exponential factor of the nucleation rate,  $k_2$ , and the density of crystals,  $\rho$ , are introduced to the system. Specifically:

$$\begin{aligned} k_2 &= k_{2,nom} + 0.5k_{2,nom}\sin(0.5t), \\ \rho &= \rho_{nom} + 0.1\rho_{nom} \end{aligned} \quad (19)$$

where  $k_{2,nom}$  and  $\rho_{nom}$  represent the nominal values of the pre-exponential factor and the crystal density respectively. The expressions of the corresponding dimensionless parameters can be obtained by substituting Eq.19 into Eq.15 to yield the following:

$$\begin{aligned} Da &= Da_{nom} + 0.5Da_{nom}\sin(0.5t), \\ \alpha &= \alpha_{nom} + 0.1\alpha_{nom} \end{aligned} \quad (20)$$

where  $Da_{nom} = 8\pi\sigma^3k_{2,nom}\tau$  and  $\alpha_{nom} = \frac{(\rho_{nom} - c_s)}{(c_0 - c_s)}$ . Substituting the formulation of the control problem of Eqs.17 and 18 into the fifth-order moment model of Eq.16, we obtain a system of the following general form:

$$\begin{aligned} \frac{d\bar{x}}{dt} &= \bar{f}(\bar{x}) + \bar{g}_1(\bar{x})\bar{u}_1 + \bar{g}_2(\bar{x})\bar{u}_2 \\ y_1 &= \bar{h}_1(\bar{x}) \quad y_2 = \bar{h}_2(\bar{x}) \end{aligned} \quad (21)$$

where  $\bar{x}$  denotes the vector  $[\bar{x}_0 \ \bar{x}_1 \ \bar{x}_2 \ \bar{x}_3 \ \bar{y}]^T$ ,  $\bar{f}(\bar{x})$ ,  $\bar{g}_1(\bar{x})$  and  $\bar{g}_2(\bar{x})$  are vector functions and  $\bar{h}_1(\bar{x})$  and  $\bar{h}_2(\bar{x})$  are scalar functions whose explicit form is omitted for brevity.

We use a method proposed in (Christofides and Daoutidis, 1997) to synthesize a robust nonlinear controller based on the model of Eq.21, of the following form:

$$\begin{aligned} \bar{u}_1(t) &= [\beta_{12}L_{\bar{g}_1}, \bar{h}(\omega)]^{-1} \{v_1 - \beta_{10}y_1 - \beta_{11}L_{\bar{f}}\bar{h}_1(\omega) \\ &\quad - \frac{-F}{|y_1 - v_1| + \phi_1} Da_0 \epsilon_{Da} [(1 - \omega_3)e^{\omega_4^2}] \} \end{aligned} \quad (22)$$

$$\bar{u}_2(t) = [\beta_{22}L_{\bar{g}_2}\bar{h}(\omega)]^{-1}\{v_2 - \beta_{20}y_1 - \beta_{21}L_f\bar{h}_2(\omega) - \frac{y_2 - v_2}{|y_2 - v_2| + \phi_2} \alpha_0 \epsilon_\alpha \left| \frac{\omega_4 \omega_2}{1 - \omega_3} \right|\} \quad (23)$$

where  $v_1$  and  $v_2$  are the set-points of the two outputs,  $\beta_{10}, \beta_{11}, \beta_{12}, \beta_{20}, \beta_{21}, \beta_{22}$  are tuning parameters.

The practical implementation of the robust nonlinear controller of Eqs.22-23 is achieved by employing the following nonlinear state observer:

$$\frac{d\omega}{dt} = \bar{f}(\omega)u + \bar{g}_1(\omega)u_1 + \bar{g}_2(\omega)u_2 + L_1(y_1 - \bar{h}_1(\omega)) + L_2(y_2 - \bar{h}_2(\omega)) \quad (24)$$

where  $\omega$  denotes the observer state vector whose dimension is equal to that of  $\bar{x}$ , and  $y_1$  and  $y_2$  are the measured outputs. The state observer of Eq.24 consists of a replica of the system of Eq.21 plus two linear gain vectors  $L_1$  and  $L_2$  multiplying the discrepancy between the actual and the estimated values of the outputs.

The performance of the nonlinear robust controller of Eqs.22-23 was tested through numerical simulations. The values of the system parameters and the ones in their corresponding dimensionless forms (Eq.15) are taken from (Chiu and Christofides, 1998) Tables 1 and 2, with the particle cut-size for the fines trap,  $r_m$  set at 1 mm. The values of the controller parameters are given as follows:  $\beta_{10} = \beta_{20} = 1, \beta_{11} = \beta_{21} = \beta_{12} = \beta_{22} = 1.5, \beta_{12}, L_1 = [1 \ 0 \ 0 \ 0 \ 0]^T, L_2 = [0 \ 0 \ 0 \ 0 \ 1]^T, \phi_1 = 9 \times 10^{-5}$  and  $\phi_2 = 9 \times 10^{-3}$ . In all simulation runs, the following initial conditions:

$$\begin{aligned} n(r, 0) &= (2.189 \times 10^3)e^{-1.168r} \text{ mm}^{-4}, \\ c(0) &= 992.1 \text{ kg m}^{-3} \end{aligned} \quad (25)$$

were used for the process model of Eq.4 and the finite difference method with 1000 discretization points was used for the simulation of Eq.4. The initial conditions for the observer states were computed numerically by using the initial conditions of Eq.25.

A simulation run was performed to evaluate the set-point tracking capabilities of the nonlinear robust multivariable controller in the presence of uncertainty. The set-points were set at  $v_1 = 0.015$  and  $v_2 = 0.5996$ . The closed-loop output profiles are shown in Figures 2 and 3 (solid lines). Clearly the controller regulates the outputs to the set-point values minimizing the effect of the time-varying uncertainty. For the sake of comparison, we also implemented the same controller without the terms responsible for the compensation of the uncertainty. Figures 2 and 3 show the closed-loop output profiles (dashed lines). It is clear that this controller cannot attenuate the effect of the uncertainty on the outputs leading to poor performance.

## 5. REFERENCES

- Chiu, T. and P.D. Christofides (1998). Nonlinear control of particulate processes. *AIChE J.* submitted.
- Christofides, P. D. and P. Daoutidis (1997). Robust control of multivariable two-time-scale nonlinear systems. *J. Proc. Contr.* 7, 313-328.

- Eaton, J. W. and J. B. Rawlings (1990). Feedback control of chemical processes using on-line optimization techniques. *Comp. Chem. Eng.* 14, 469-479.
- Hulburt, H. M. and S. Katz (1964). Some problems in particle technology: A statistical mechanical formulation. *Chem. Eng. Sci.* 19, 555-574.
- Lei, S. J., R. Shinnar and S. Katz (1971). The stability and dynamic behavior of a continuous crystallizer with a fines trap. *AIChE J.* 17, 1459-1470.
- Randolph, A. D. and M. A. Larson (1988). *Theory of Particulate Processes*. Academic press, Second edition. San Diego.
- Rawlings, J. B., S. M. Miller and W. R. Witkowski (1993). Model identification and control of solution crystallization processes. *I & EC Res.* 32, 1275-1296.
- Rohani, S. and J. R. Bourne (1990). Self-tuning control of crystal size distribution in a cooling batch crystallizer. *Chem. Eng. Sci.* 12, 3457-3466.
- Semino, D. and W. H. Ray (1995a). Control of systems described by population balance equations-I. controllability analysis. *Chem. Eng. Sci.* 50, 1805-1824.
- Semino, D. and W. H. Ray (1995b). Control of systems described by population balance equations-II. emulsion polymerization with constrained control action. *Chem. Eng. Sci.* 50, 1825-1839.

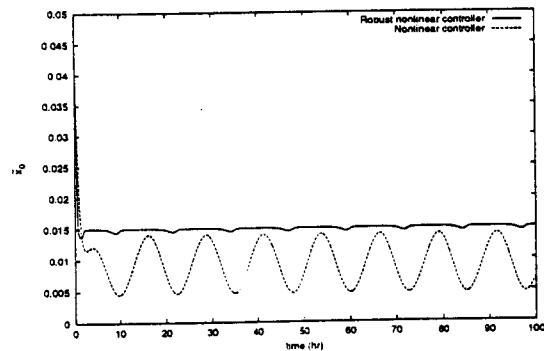


Fig. 2. Closed-loop output profiles for  $\bar{x}_0$  under robust nonlinear controller (solid line) and nonlinear controller which does not account for uncertainty (dashed line).

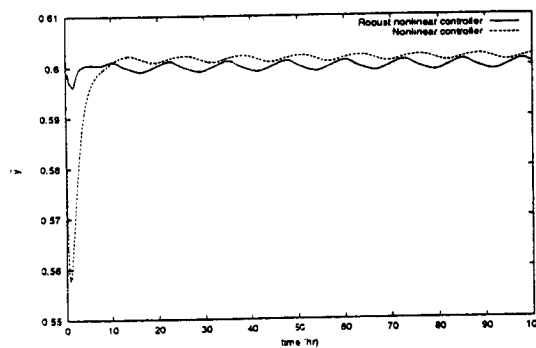


Fig. 3. Closed-loop output profiles for  $\bar{y}$  under robust nonlinear controller (solid line) and nonlinear controller which does not account for uncertainty (dashed line).